Proceedings of the ASME 2011 International Design Engineering Technical Conferences & Computers and Information in Engineering Conference
IDETC/CIE 2011
August 28-31, 2011, Washington, DC, USA

DETC2011-48816

A Parallel GPU Implementation of the Absolute Nodal Coordinate Formulation with a Frictional/Contact Model for the Simulation of Large Flexible Body Systems

Naresh Khude
Dept. of Mechanical Engineering
University of Wisconsin – Madison
Madison, WI 53706

Dan Melanz
Dept. of Mechanical Engineering
University of Wisconsin – Madison
Madison, WI 53706

Ilinca Stanciulescu
Department of Civil and Environmetal Engineering
Rice University
Houston, TX 77005

Dan Negrut
Dept. of Mechanical Engineering
University of Wisconsin – Madison
Madison, WI 53706

ABSTRACT
This contribution discusses how a flexible body formalism, specifically, the Absolute Nodal Coordinate Formulation (ANCF), is combined with a frictional/contact model using the Discrete Element Method (DEM) to address many-body dynamics problems; i.e., problems with hundreds of thousands of rigid and deformable bodies. Since the computational effort associated with these problems is significant, the analytical framework is implemented to leverage the computational power available on today's commodity Graphical Processing Unit (GPU) cards. The code developed is validated against ANSYS and FEAP results. The resulting simulation capability is demonstrated in conjunction with hair simulation.

THEORETICAL BACKGROUND - ANCF
For almost a decade the Absolute Nodal Coordinate formulation (ANCF) has been widely used to carry out the dynamics analysis of flexible bodies that undergo large rotation and large deformation. This formulation is consistent with the nonlinear theory of continuum mechanics and easy to implement. Also, it leads to a constant mass matrix which makes it computationally more efficient compared to other nonlinear finite element formulations.

The fully parameterized ANCF beam element was originally introduced in [1]. The locking problems of Fully Parameterized ANCF finite elements based on the continuum mechanics approach have been addressed in the literature [2, 3]. These locking problems significantly deteriorate the performance of ANCF finite elements especially for the thin and stiff structures. Since the main focus of this work is to simulate the frictional contact problem between several slender beams, the original ANCF beam elements were not a good choice for this problem. Instead, the gradient deficient ANCF 3D beam elements, also referred as low order cable elements in [3, 4] are used to model the slender beams. These are two node beam elements where one position vector and only one gradient vector are used as nodal coordinates $\mathbf{e}_i = [\mathbf{r}^T \ \mathbf{r}_x^T]^T$. Thus each node has 6 coordinates: three components of global position vector of the node and three components of position vector gradient at the node. It should be noted that the gradient deficient ANCF beam element does not describe a rotation of beam about its own axis so the torsional effects cannot be modeled [3]. However, this formulation shows no shear locking problems for thin and stiff beams and it is computationally efficient compared to the original ANCF due to reduced nodal coordinates.

The global position vector of an arbitrary point on the beam centerline is given by

$$\mathbf{r}(x,\mathbf{e}) = \mathbf{S}(x)\mathbf{e} \quad (1)$$

where $\mathbf{e} = \left[\mathbf{e}_1^T \ \mathbf{e}_2^T\right]^T \in \mathbb{R}^{12}$ is the vector of element nodal coordinates. The shape function matrix for this element is defined as $\mathbf{S} = [S_1\mathbf{I}\ S_2\mathbf{I}\ S_3\mathbf{I}\ S_4\mathbf{I}\ ] \in \mathbb{R}^{3\times 12}$ where $\mathbf{I}$ is the 3×3 identity matrix and the shape functions $S_j,\ j = 1,\ldots,4$ are defined as [4]

$$\begin{aligned} s_1 &= 1 - 3\xi^2 + 2\xi^3, \quad s_2 = l(\xi - 2\xi^2 + \xi^3) \\ s_3 &= 3\xi^2 - 2\xi^3, \quad s_4 = l(-\xi^2 + \xi^3) \end{aligned} \tag{2}$$

where $\xi = x / l$, and l is the element length. Using the principle of virtual work for the continuum, the element equation of motion is obtained as:

$$\mathbf{M}\ddot{\mathbf{e}} + \mathbf{Q}_s = \mathbf{Q}_e \tag{3}$$

where $\mathbf{Q}_s$ is the vector of generalized element elastic forces, $\mathbf{Q}_e$ is the vector of generalized element external forces, and $\mathbf{M}$ is the symmetric consistent element mass matrix defined as

$$\mathbf{M} = A\int_0^l \rho\mathbf{S}^T\mathbf{S}\,dx \tag{4}$$

Here ρ and A are the element mass density and cross sectional area, respectively**.** The expression for the mass matrix given in (4) is derived using the virtual work of the inertia forces. Note that the element mass matrix is not a function of the time-dependent nodal coordinates.

The generalized element external force vector ($\mathbf{Q}_e \in \mathbb{R}^{12}$) due to gravity can be obtained as

$$\mathbf{Q}_e = A\int_0^l \mathbf{S}^T\mathbf{f}_g\,dx \tag{5}$$

where $\mathbf{f}_g = [0, -\rho g, 0]^T$ is the gravity force vector considering Y as the vertical axis. If a concentrated/point force is applied to an element at some point, the generalized element external force vector ($\mathbf{Q}_e \in \mathbb{R}^{12}$) in this case is obtained using the principle of virtual work as

$$\mathbf{Q}_e = \mathbf{S}^T\mathbf{f} \tag{6}$$

where $\mathbf{f}$ is an external point force and $\mathbf{S}$ is the shape function matrix defined at the point of application of the force.

The strain energy expression for the gradient deficient ANCF beam element is

$$U = \frac{1}{2}\int_0^l EA(\varepsilon_{11})^2\,dx + \frac{1}{2}\int_0^l EI(\kappa)^2\,dx \tag{7}$$

where $\varepsilon_{11} = \frac{1}{2}\ \mathbf{r}_x^T\mathbf{r}_x - 1$ is the axial strain and the magnitude of curvature vector κ is given as [4]

$$\kappa = \frac{\left|\mathbf{r}_x \times \mathbf{r}_{xx}\right|}{\left|\mathbf{r}_x\right|^3} \tag{8}$$

The vector of the element elastic forces ($\mathbf{Q}_s \in \mathbb{R}^{12}$) is determined from the strain energy expression as

$$\mathbf{Q}_s = \int_0^l EA(\varepsilon_{11})\left(\frac{\partial\varepsilon_{11}}{\partial\mathbf{e}}\right)^T dx + \int_0^l EI(\kappa)\left(\frac{\partial\kappa}{\partial\mathbf{e}}\right)^T dx \tag{9}$$

For the gradient deficient ANCF beam element the equation of motion and the expressions for element mass matrix and element external force are the same as in case of a fully parameterized ANCF beam element. Computing the element elastic force is much easier in this case. Since in the shape functions only one spatial coordinate (ξ) is used, the numerical integration is carried out using the Gauss-quadrature formula in one dimension only.

THEORETICAL BACKGROUND - DEM

The Discrete Element Method (DEM) was proposed by Cundall to model the mechanical behavior of granular material [5, 6]. The DEM can be classified as a penalty method, where the force acting between two colliding bodies is computed based on the associated interpenetration. DEM approaches have been widely used in rock mechanics, molecular dynamics, and granular dynamics simulation. The basic idea behind the DEM frictional contact model is to introduce a fictitious spring-damper element that is placed between two bodies when they collide. The spring and damping coefficients can be derived from the continuum theory [7] or calibrated based on experimental data. The schematic of DEM contact is shown in Figure 1.

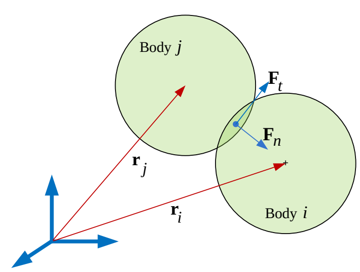

Figure 1. Schematic of DEM contact

Numerous contact force models have been developed over the past decades [8-11]. This paper uses the volumetric-based Coulomb friction contact model introduced in [12]. In this model, the normal contact force $\mathbf{F}_n$ is given as

$$\mathbf{F}_n = \frac{k_f}{h_f}V(1 + a\mathbf{v}_{cn})\boldsymbol{n} \tag{10}$$

where k_f and h_f are the elastic modulus and depth of the Winkler elastic foundation [12], respectively; $\mathbf{v}_{cn}$ is the relative velocity of colliding sphere in normal ($\boldsymbol{n}$) direction; V is total penetration volume, and the damping term a is a function of the coefficient of restitution and of the initial impact velocity, see [13]. The friction model presented in [13] is used where the Coulomb friction force $\mathbf{F}_t$ is given as

$$\mathbf{F}_t = -\mu_c \mathbf{F}_n dir_\varepsilon(\mathbf{v}_{ct}, \upsilon_\varepsilon) \tag{11}$$

where μ_c is the Coulomb friction coefficient, $\mathbf{v}_{ct}$ is the relative tangential velocity of colliding spheres, υ_ε is a velocity tolerance, and the term $dir_\varepsilon(\mathbf{v}_{ct}, \upsilon_\varepsilon)$ is defined as

$$dir_\varepsilon(\mathbf{v}_{ct}, \upsilon_\varepsilon) = \begin{cases} \dfrac{\mathbf{v}_{ct}}{\left|\mathbf{v}_{ct}\right|}; & \left|\mathbf{v}_{ct}\right| \geq \upsilon_\varepsilon \\ \dfrac{\mathbf{v}_{ct}}{\upsilon_\varepsilon}\left(\dfrac{3}{2}\dfrac{\left|\mathbf{v}_{ct}\right|}{\upsilon_\varepsilon} - \dfrac{1}{2}\left(\dfrac{\left|\mathbf{v}_{ct}\right|}{\upsilon_\varepsilon}\right)^3\right); & \left|\mathbf{v}_{ct}\right| < \upsilon_\varepsilon \end{cases} \tag{12}$$

The DEM approach can be easily implemented with the explicit numerical integration method; however, it requires a very small integration step-size to maintain the stability and accuracy of the numerical solution. The integration step size depends on the size of spheres, the material properties associated with the bodies in contact, and the relative velocity of the spheres. Because of the rigid body assumptions, the stiff springs enter into the DEM model which leads to high transients and instability of numerical integration. In this paper the symplectic Euler integration method is used for the simulation as it is more stable than the regular forward Euler method.

IMPLEMENTATION OF ANCF AND DEM

In DEM the colliding bodies are assumed to be rigid. To extend this approach for the frictional contact between slender beams, a spherical decomposition of the colliding beams is implemented in this paper. Specifically, as shown in Figure 2, each flexible beam can be considered as a chain of spheres that overlap and which are distributed equally along the axis of the gradient deficient ANCF beam elements. At each time step the collision detection between the spheres in all the beams is performed and the normal and tangential contact forces between the colliding spheres are calculated using DEM. The spherical decomposition approach along with DEM provides the magnitude and direction of the contact force and its location relative to the beam element. These contact forces are treated as externally applied point forces in the nonlinear dynamics analysis with ANCF. For thin beams the moments of tangential/frictional contact forces about the beam centerline can be neglected. It should be noted that this approach allows multiple contacts between the colliding beams and also self-contact in case of a long, highly deformable beam.

The spherical decomposition approach simplifies the process of collision detection between the slender beams. The collision detection problem can be a bottleneck in the simulation of physical systems involving a large number of many bodies. For the hair simulation problem one has to consider the systems with tens of thousands of flexible beams interacting through friction and contact for which the collision detection between millions of spheres needs to be done at each time step. A parallel implementation on the GPU provides significant speed up for such a problem.

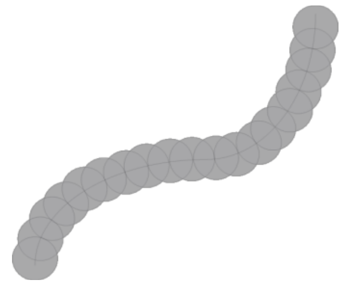

Figure 2. Spherical decomposition along the centerline of deformed beam

Being computationally very intensive, the DEM and ANCF methodologies stand to benefit from the use of parallel computation. In the simulation of complex mechanical systems with many flexible beams (e.g. hair or polymer simulation), the equations of motion of each beam can be solved in parallel. The computation of the nonlinear internal force and the external force can also be done in parallel at element level. All these aspects are anticipated to lead to significant reductions in simulation times for large flexible body systems.

Collision Detection Example

A first set of numerical experiments gauged the efficiency of the parallel collision detection algorithm developed. The reference used was a *sequential* implementation from Bullet Physics Engine, an open source physics-based simulation engine [14]. The CPU used in this experiment (relevant for the Bullet results) was AMD Phenom II Black X4 940, a quad core 3.0 GHz processor that drew on 16 GB of RAM. The GPU used was NVIDIA's Tesla C1060. The operating system used was the 64-bit version of Windows 7. The test was meant to gauge the relative speedup gained with respect to the serial implementation. This test stopped when dealing with about six million contacts (see horizontal axis of Figure 3), when Bullet ran into memory management issues. The plot illustrates a 180 fold relative speedup when going from sequential Bullet to the in-house developed GPU-based parallel implementation.

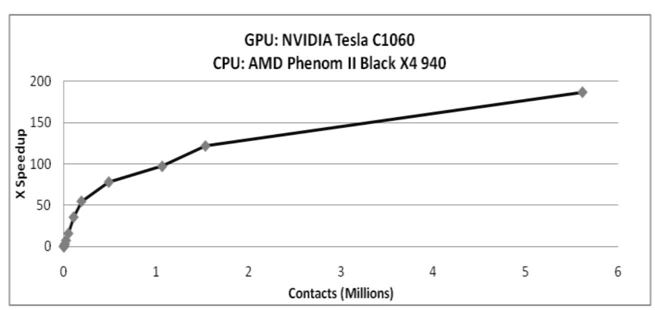

Figure 3.Overall speedup when comparing the CPU algorithm to the GPU algorithm. The maximum speedup achieved was approximately 180 times [15].

NUMERICAL EXPERIMENTS AND RESULTS

Several numerical experiments are carried out in order to *a)* Validate the gradient deficient ANCF against FEAP and ANSYS; *b)* Compare the gradient deficient ANCF beam elements against fully parameterized ANCF beam elements; *c)* Assess the potential of the ANCF and DEM implementation: *d)* Carry out a convergence analysis of the gradient deficient ANCF beam elements; *e)* Assess the computation time-speedup obtained due to the parallel GPU implementation.

The details of the models used in the numerical experiments and the simulation parameters are given in Table 1. For all the numerical experiments the flexible pendulums/beams are assumed to be in horizontal configuration initially with no initial velocity.

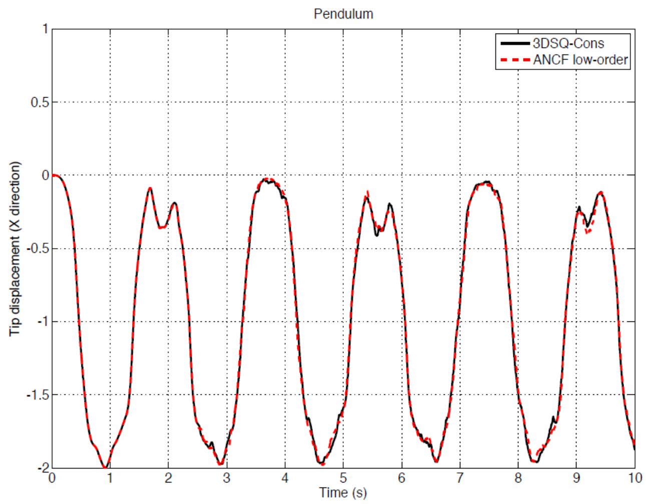

Figure 4. X displacement of a pendulum-tip (ANCF and FEAP comparison)

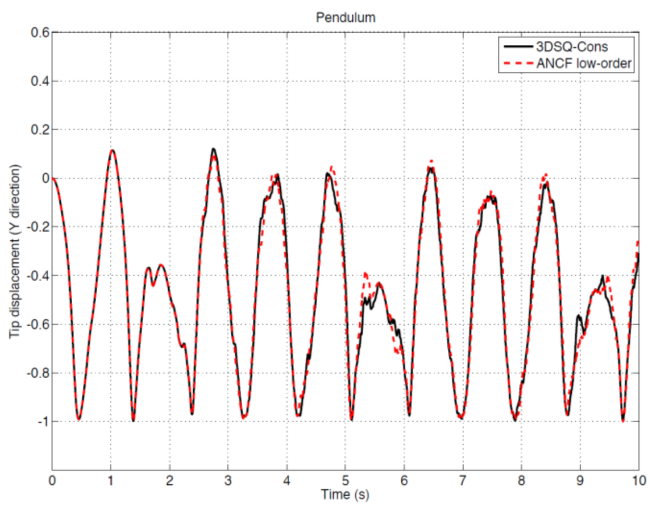

Figure 5. Y displacement of a pendulum-tip (ANCF and FEAP comparison)

Table 1. The model and simulation parameters

Parameters	Model 1	Model 2	Model 3
Length (m)	1	1	3
Cross-section Area(m^2)	0.02 x 0.02	π x 0.01^2	π x 0.01^2
Material Density (kg/ m^3)	7200	7200	7200
Modulus of elasticity (Pa)	2.0E7	2.0E7	2.0E7
Second moment of inertia (m^4)	1.33E-8	7.85E-10	7.85E-10
Tip Mass (kg)	--	--	5
Number of 3D beam elements	4	1	8
External Force	Gravity	Gravity + Contact	Gravity + Contact
Numerical Integrator	Symplectic Euler	Symplectic Euler	Symplectic Euler
Integration Step-size	1.0E-4	1.0E-4	1.0E-4

Validation of the gradient deficient ANCF elements

Model 1 is used to study the motion of a highly deformable 3D pendulum (beam pinned at one end) under the effect of gravity. The pendulum tip displacements are compared with those using 40 solid elements (27-node) in FEAP. Figure 4 and Figure 5 show that the results are in good agreement and the gradient deficient ANCF beam elements do not suffer from shear locking problems. The symplectic Euler integrator with the step size of 1.0E-4 *sec* is used in this simulation. Figure 6 shows the total energy using gradient deficient ANCF remains constant as the system is conservative. It also shows that the explicit integration scheme used in this simulation remains stable. The tip displacements of the flexible pendulum are compared with those obtained using fully parameterized ANCF beam elements. Figure 7 and Figure 8 show considerable difference between the two results which is attributed to the locking problem of original ANCF beam elements in case of thin beams. Model 1 is also used for nonlinear dynamics analysis in ANSYS using BEAM4 elements. From Figure 9 it is observed that the implicit integration with step size of 1.0E-3 *sec* used in ANSYS does not converge for Model 1 when 8 and 16 elements are used. Thus ANSYS requires more number of beam elements for the solution to converge. The ANSYS results using 64 BEAM4 elements are compared with those using 16 gradient deficient ANCF beam elements in Figure 10. The difference in the results shows that the large deformations of thin beams cannot be modeled correctly with BEAM4 elements (nonlinear option) in ANSYS.

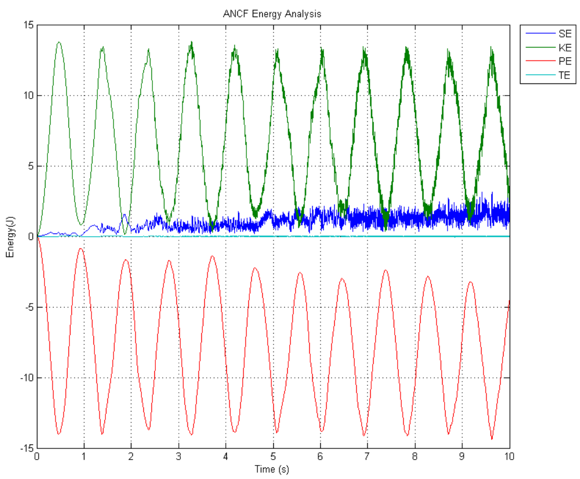

Figure 6. Energy Analysis – GD ANCF (SE: strain energy, KE: kinetic energy, PE: potential energy, TE: total energy)

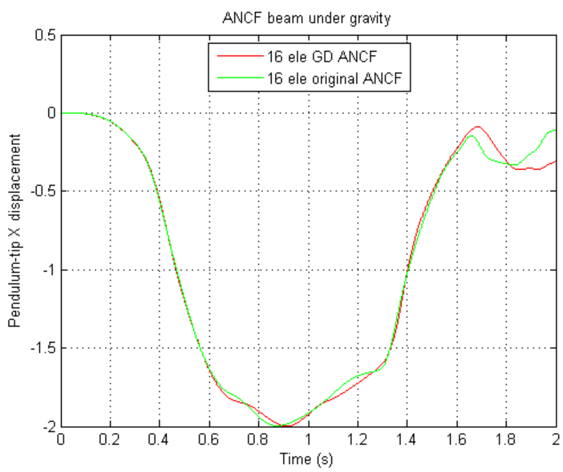

Figure 7. X displacement of a pendulum-tip (ANCF and GD ANCF comparison)

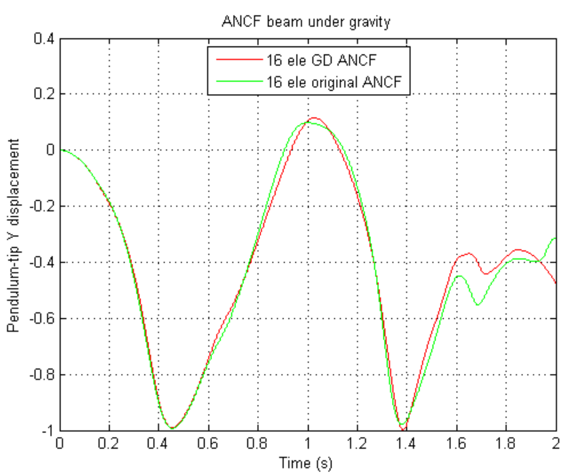

Figure 8. Y displacement of a pendulum-tip (ANCF and GD ANCF comparison)

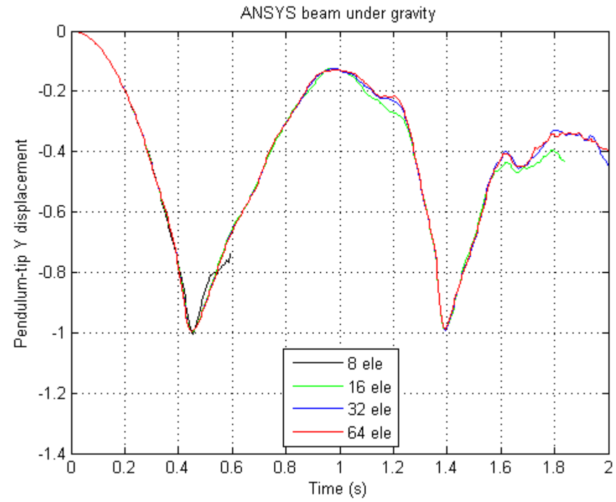

Figure 9. Y displacement of a pendulum-tip using ANSYS

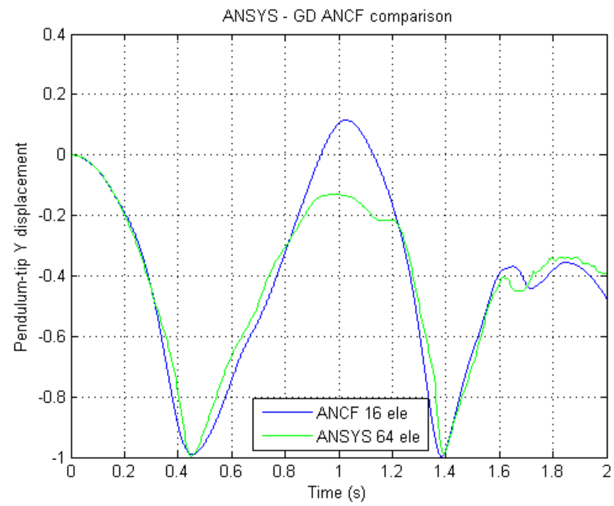

Figure 10. Y displacement of a pendulum-tip (ANSYS and GD ANCF comparison)

ANCF with frictional contact

In the second set of numerical experiments the frictional contact phenomenon between two flexible beams (pinned at one end) is studied using Model 2. For the contact force model, the Coulomb friction coefficient $\mu_c = 0.3$ is used. The damping factor a was selected to obtain a coefficient of restitution of 0.975 so that small amount of energy is dissipated through damping. The contact stiffness k_f / h_f used in this model is 2.0E9 N/m. Snapshots of the numerical simulation of this model are shown in Figure 11.

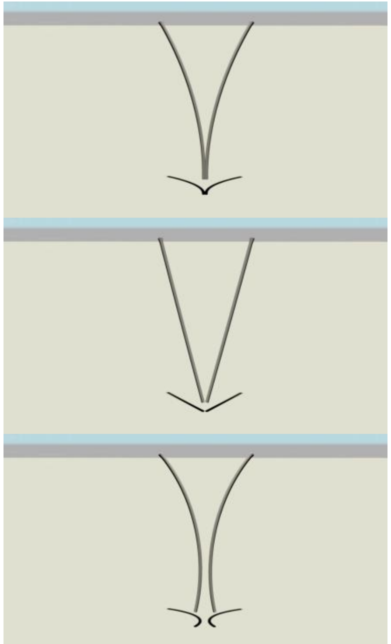

Figure 11. Snapshots from simulation of Model 2

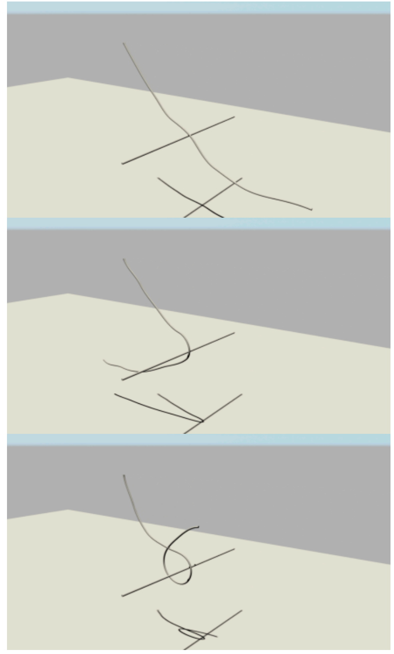

Figure 12. Snapshots from simulation of Model 3

Model 3 is used to simulate the frictional contact between a long flexible beam (pinned at one end) with a tip mass and a rigid cylinder. Figure 12 shows a sequence of three snapshots of the numerical simulation of this model. It should be noted that the DEM approach used in this paper allows the contact force modeling between the rigid bodies and the flexible beams. Figure 13 shows the snapshots of simulation of 8 instances of Model 3. In this parametric study, the number of elements varied in each beam from one element to eight elements. A rigid horizontal cylinder with radius of 0.01 m was fixed at position (1, -1.5) so that the elements would come into contact with the rigid cylinder as they moved. The beams tend to wrap around the rigid cylinder due to inertia of the tip mass. The overall bending stiffness of the beam tends to decrease as the number of elements increases and hence different trajectories of the beam tip are observed, as seen in Figure 13. The videos of these simulations are available at [16].

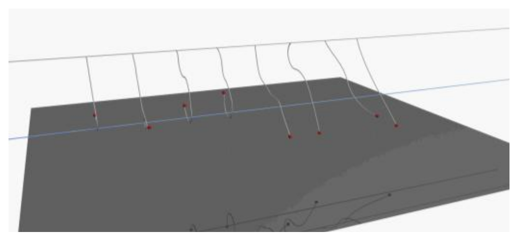

Figure 13. Snapshot from parametric study of model 3

Convergence analysis of ANCF and DEM

In order to investigate the convergence of the gradient deficient ANCF elements a Model 2 beam (pinned at one end) with a tip-mass of 1kg is used in this analysis. The beam is modeled using various numbers of elements and the pendulum tip positions are compared for a 4 *sec* long simulation. Figure 14 and Figure 15 show that as the number of elements is increased, the results tend to converge to a single value. The gradient deficient ANCF beam elements exhibit good convergence characteristics. Thus the large deformation of slender beams can be effectively modeled with very few gradient deficient ANCF beam elements.

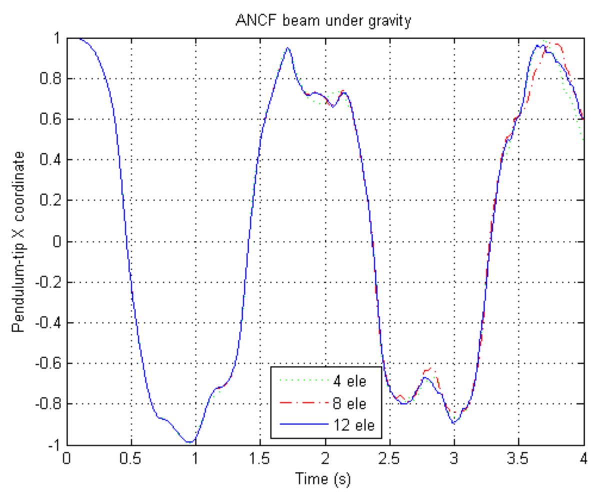

Figure 14. X coordinate of a pendulum-tip (non-contact case)

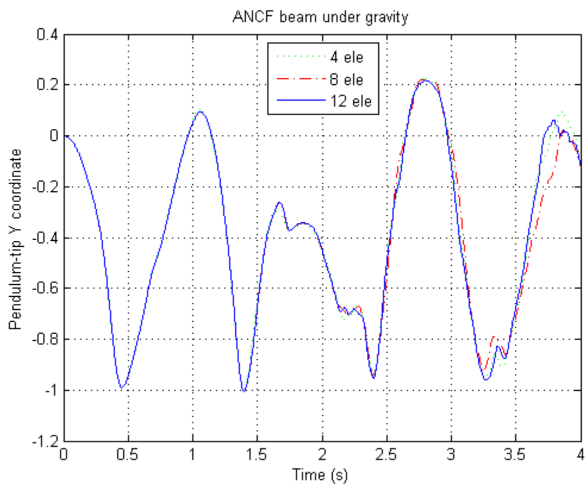

Figure 15. Y coordinate of a pendulum-tip (non-contact case)

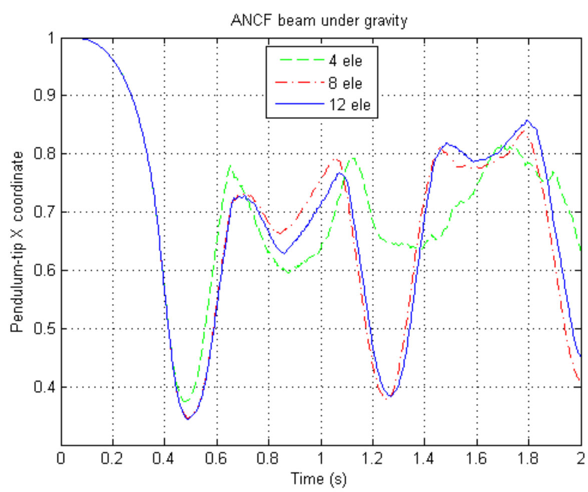

Figure 16. X coordinate of a pendulum-tip (contact case)

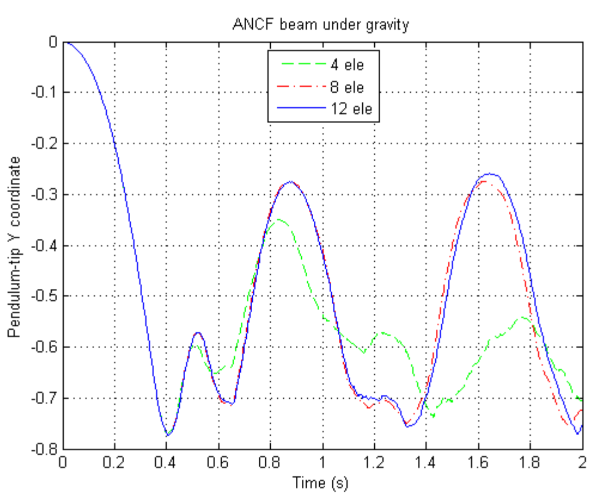

Figure 17. Y coordinate of a pendulum-tip (contact case)

It is also important to investigate the convergence characteristics of the ANCF with frictional contact. In this analysis the same model is used which comes into contact with the rigid cylinder fixed at position (0.5, -0.5). From Figure 16 and Figure 17, it can be seen that the pendulum tip displacements tend to converge as the number of elements is increased, which shows that the convergence characteristics of ANCF are not affected when combined with DEM approach.

Comparison of GPU and CPU computation times

In this simulation a complex mechanical system containing hundreds of thousands of flexible beams pinned at one end and with different initial conditions is used. Model 3 beams with 8 elements are used in this analysis. It is assumed that the beams do not come into contact with each other. Several instances of the CPU and GPU implementations were run on an Intel Nehalem Xeon E5520 2.26GHz processor with an NVIDIA Tesla C1060 graphics card for varying numbers of beams. On average, a 15x speedup was observed from the GPU implementation over the CPU implementation, shown in Figure 18.

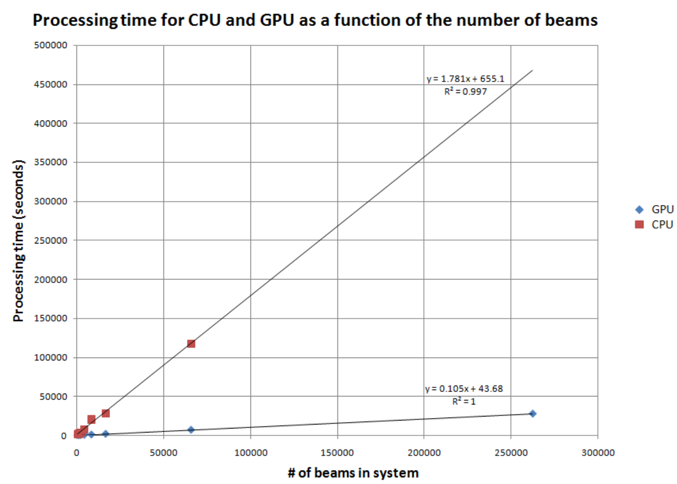

Figure 18. Processing time for the CPU and GPU implementations for varying numbers of beams.

CONCLUSIONS

This paper presents a methodology for combining DEM with ANCF to model the frictional contact between highly deformable thin beams. The gradient deficient ANCF beam elements used in the dynamics analysis exhibit good convergence characteristics and do not suffer from shear locking problems. The dynamics analysis results of thin beams are validated against FEAP and compared with ANSYS results.

A spherical decomposition approach is used to simplify the contact detection between beams. Both the DEM and ANCF methodologies stand to benefit from the use of parallel computation. The potential of parallel computation at the element level and at the body level in ANCF has been investigated and shown to lead on average to a 15 fold speedup when drawing on GPU computing.

The scaling results for systems with hundreds of thousands of flexible bodies (e.g., hair or polymer simulation) show that the GPU simulation approach proposed has the potential to increase the relevance of flexible multibody dynamics in addressing challenging real-life design problems across a spectrum of engineering disciplines.

ACKNOWLEDGEMENTS

The last author was financially supported in part by the National Science Foundation grant NSF-CMMI-0840442 and Function Bay, Inc.

REFERENCES

[1] Shabana, A. and R. Yakoub, *Three dimensional absolute nodal coordinate formulation for beam elements: Theory.* Journal of Mechanical Design, 2001. **123**: p. 606.

[2] Schwab, A. and J. Meijaard. *Comparison of three-dimensional flexible beam elements for dynamic analysis: finite element method and absolute nodal coordinate formulation*. in *Proceedings of the ASME 2005 IDETC/CIE*. November 5- 11, 2005. Orlando, Florida.

[3] Gerstmayr, J. and A. Shabana, *Analysis of thin beams and cables using the absolute nodal co-ordinate formulation.* Nonlinear Dynamics, 2006. **45**(1): p. 109-130.

[4] Shabana, A.A., *Computational continuum mechanics*. 2008: Cambridge University Press, New York.

[5] Cundall, P. and O. Strack, *A discrete element model for granular assemblies.* Geotechnique, 1979. **29**(1): p. 47-65.

[6] Cundall, P., *A Computer Model for Simulating Progressive, Large Scale Movements in Blocky Rock Systems. Symp.* Int. Soc. Rock Mechanics, Nancy, 1971.

[7] Johnson, K.L., *Contact Mechanics*. 1987, Cambridge: University Press.

[8] Rapaport, D., *Simulational studies of axial granular segregation in a rotating cylinder.* Physical Review E, 2002. **65**(6): p. 61306.

[9] Rapaport, D., *Radial and axial segregation of granular matter in a rotating cylinder: A simulation study.* Physical Review E, 2007. **75**(3): p. 31301.

[10] Silbert, L., D. Erta , G. Grest, T. Halsey, D. Levine, and S. Plimpton, *Granular flow down an inclined plane: Bagnold scaling and rheology.* Physical Review E, 2001. **64**(5): p. 51302.

[11] Landry, J., G. Grest, L. Silbert, and S. Plimpton, *Confined granular packings: structure, stress, and forces.* Physical Review E, 2003. **67**(4): p. 41303.

[12] Gonthier, Y., J. McPhee, and C. Lange. *On the implementation of coulomb friction in a volumetric-based model for contact dynamics*. in *Proceedings of the ASME 2007 IDETC/CIE*. September 4-7, 2007. Las Vegas, NV.

[13] Gonthier, Y., J. McPhee, C. Lange, and J. Piedboeuf, *A regularized contact model with asymmetric damping and dwell-time dependent friction.* Multibody System Dynamics, 2004. **11**(3): p. 209-233.

[14] Erwin, C. *Physics Simulation Forum*. 2010 [cited 2010 January 15]; Available from: http://www.bulletphysics.com/Bullet/wordpress/.

[15] Mazhar, H., T. Heyn, and D. Negrut, *Large Scale Parallel Collision Detection on the Graphics Processing Unit.* Multibody System Dynamics, under review, 2010.

[16] SBEL. *Simulation-Based Engineering Lab, Department of Mechanical Engineering, University of Wisconsin, Madison: http://sbel.wisc.edu/Animations/index.htm*. 2010 [cited 2010 January 27].